The paradox of assessing greenhouse gases from soils for nature-based solutions

Authors:

Rodrigo Vargas[1*] and Van Huong Le[1]

Affiliations

[1]Department of Plant and Soil Science, University of Delaware, Newark, DE, USA

*Corresponding Author

Rodrigo Vargas (rvargas@udel.edu)

Abstract

Quantifying the role of soils in nature-based solutions requires accurate estimates of soil greenhouse gas (GHG) fluxes. Technological advances allow us to measure multiple GHGs simultaneously, and now it is possible to provide complete GHG budgets from soils (i.e., CO_2, CH_4, and N_2O fluxes). We propose that there is a conflict between the convenience of simultaneously measuring multiple soil GHG fluxes at fixed time intervals (e.g., once or twice per month) and the intrinsic temporal variability and patterns of different GHG fluxes. Information derived from fixed time intervals -commonly done during manual field campaigns- had limitations to reproducing statistical properties, temporal dependence, annual budgets, and associated uncertainty when compared with information derived from continuous measurements (i.e., automated hourly measurements) for all soil GHG fluxes. We present a novel approach (i.e., temporal univariate Latin Hypercube sampling) that can be applied to provide insights and optimize monitoring efforts of GHG fluxes across time. We suggest that multiple GHG fluxes should not be simultaneously measured at a few fixed time intervals (mainly when measurements are limited to once per month), but an optimized sampling approach can be used to reduce bias and uncertainty. These results have implications for assessing GHG fluxes from soils and consequently reduce uncertainty on the role of soils in nature-based solutions.

Keywords: Carbon dioxide, methane, nitrous oxide, representativeness, uncertainty

1. Introduction

Soils are essential for nature-based solutions for their role in climate mitigation potential through implementing different natural pathways (Griscom et al., 2017; Bossio et al., 2020). The climate mitigation potential of soils is dependent on multiple factors such as weather variability (Kim et al., 2012), ecosystem type (Oertel et al., 2016), soil structure (Ball, 2013), management practices (Shakoor et al., 2021), or disturbances (Vargas, 2012), where soils can ultimately act as net sources or sinks of greenhouse gases (GHGs). Therefore, accurate quantification of the magnitudes and patterns of soil GHGs fluxes is needed to understand the potential of soils to mitigate or contribute to global warming across ecosystems and different scenarios.

Most of our understanding of soil GHGs has come from manual measurements performed throughout labor-intensive field campaigns and experiments (Oertel et al., 2016). While most studies around the world have focused on soil CO_2 fluxes (Jian et al., 2020), early examples have reported coupled measurements of soil CO_2, CH_4, and N_2O fluxes across tropical forests (Keller et al., 1986) and savannas (Hao et al., 1988), temperate forests (Bowden et al., 1993), and peatlands (Freeman et al., 1993). These pioneer studies provided an early view of the importance of integrated measurements of multiple soil GHG fluxes to understand the net global warming potential of soils but also demonstrated the technical limitations and challenges associated with these efforts. For example, it is known that manual measurements have the strength of providing good spatial coverage during field surveys but provide limited information about the temporal variability (Yao et al., 2009; Barba et al., 2021).

Technological advances have opened the opportunity to simultaneously measure multiple soil GHG fluxes (i.e., CO_2, CH_4, and N_2O) at unprecedented temporal resolution (e.g., hourly). These efforts have demonstrated differences in diel patterns and pulse events

65 (e.g., rewetting) due to wetting and drying cycles across tropical (Butterbach-Bahl et al.,
66 2004; Werner et al., 2007), subtropical (Rowlings et al., 2012), and temperate (Savage et al.,
67 2014; Petrakis et al., 2017) ecosystems. These approaches provide more accurate information
68 to calculate net GHG budgets and the global warming potential of soils (Capooci et al.,
69 2019). That said, performing automated measurements of multiple GHGs is expensive, and
70 this approach usually has a lower representation of the spatial heterogeneity within
71 ecosystems (Yao et al., 2009; Barba et al., 2021).

72 Ideally, we would like to measure everything, everywhere, and all the time, but this is
73 impossible due to logistical, technological, physical, and economic constraints. Lightweight
74 and low-powered laser-based spectrometers have reduced technical barriers to
75 simultaneously measuring multiple GHGs fluxes from soils. It is now easier and faster to
76 perform discrete manual surveys across time. This opportunity creates a paradox concerning
77 when to measure different GHG fluxes from soils when performing manual measurements.
78 Researchers generally tend to perform simultaneous measurements of multiple GHGs during
79 manual surveys, but this convenience could result in biased information. We propose that
80 there is a conflict between the convenience of measuring multiple GHGs at a few fixed time
81 intervals and the intrinsic temporal variability of magnitudes and patterns of different GHG
82 fluxes.

83 Here, we present a proof-of-concept and test how a subset of measurements derived
84 from a fixed temporal stratification (FTS) for simultaneous measurements (i.e., stratified
85 sampling schedule) or using an optimized sampling (i.e., temporal univariate Latin
86 Hypercube sampling (*tuLHs*)), compared with automated measurements of soil CO_2 (F_ACO_2),
87 CH_4 (F_ACH_4), and N_2O (F_AN_2O) fluxes from a temperate forest (Petrakis et al., 2018; Barba
88 et al., 2021, 2019). The underlying assumption supporting any FTS approach is that a few
89 measurements in time can reproduce the statistical properties and temporal dependencies of

soil CO_2, CH_4, and N_2O fluxes because these GHGs respond similarly to biological and physical drivers. The *tuLHs* is a new optimization approach to reproduce the probability distribution and the temporal dependence of each original time series of GHG fluxes. We reveal that reporting GHG fluxes using an FTS for simultaneous measurements may result in biased information on temporal patterns and magnitudes. This study shows how a biased sampling schedule could influence our understanding of GHG fluxes and, ultimately, the climate mitigation potential of soils.

2. Materials and Methods

2.1 Study site

The experiment was performed in a temperate forest located at the St Jones Estuarine Reserve (a component of the Delaware National Estuarine Research Reserve [DNERR] in Delaware, USA. The site has a mean annual temperature of 13.3 °C and a mean annual precipitation of 1119 mm. Soils are classified as Othello silt loam with a texture of 40% sand, 48% silt, and 12% clay within the first 10 cm (Petrakis et al., 2018). The dominant plant species are bitternut hickory (*Carya cordiformis*), eastern red cedar (*Juniperus virginiana* L.), American holly (*Ilex opaca*), sweet gum (*Liquidambar styraciflua* L.), and black gum (*Nyssa sylvatica* (Marshall)). The site has a mean tree density of 678 stems ha^{-1} and a diameter at breast height (DBH) of 25.7±13.9 cm (mean±SD) (Barba et al., 2021).

2.2 Automated measurements of soil GHG fluxes

We analyzed data from automated measurements (1hr time intervals) of soil emissions of three GHGs (i.e., CO_2, CH_4, and N_2O) between January and December 2015. This was a typical year with a mean annual temperature of 13.4 °C and an annual precipitation of 1232 mm. Continuous measurements of soil GHGs were taken by coupling a closed-path infrared

gas analyzer (Li-COR LI-8100 A, Lincoln, Nebraska) and nine dynamic soil chambers (Li-COR 8100–104) controlled by a multiplexer (Li-COR 8100-104) with a cavity ring-down spectrometer (Picarro G2508, Santa Clara, California). A detailed description of the experimental design and measurements protocol is described in previous studies (Petrakis et al., 2018; Barba et al., 2021, 2019). Briefly, for each flux observation, we measured CO_2, CH_4, and N_2O concentrations every second with the Picarro G2508 for 300 seconds and calculated fluxes (at 1 hr time intervals) from the mole dry fraction of each gas (i.e., corrected for water vapor dilution) using the SoilFluxPro software (v4.0; Li-COR, Lincoln, Nebraska, USA). Fluxes were estimated using linear and exponential fits, and we kept the flux calculation with the highest R^2. We applied quality assurance and quality control protocols using information from all three GHGs as established in previous studies (Petrakis et al., 2018; Barba et al., 2021, 2019; Capooci et al., 2019; Petrakis et al., 2017). Using these time series, we extracted values to represent discrete temporal measurements based on FTS and used the optimization approach described below.

2.3 Temporal subsampling of time series

Subsampling of time series was performed using FTS and a temporal optimization following a univariate Latin Hypercube (*tuLHs*) approach. The difference between FTS and temporal optimization is that the first approach is focused on a fixed schedule (e.g., sampling once per month), and the second is focused on reproducing the statistical properties and temporal dependence relationship of the original GHG time series with a subset of measurements. This means optimized subsamples may not be spaced systematically (e.g., every 15 days), and selected dates may vary for each GHG flux due to their specific statistical properties and temporal dependence.

FTS represents a traditional schedule for performing manual measurements of GHG fluxes from soils. The FTS is usually performed with manual measurements because they require extensive logistical coordination due to travel time and costs, availability of instrumentation (e.g., gas analyzers), personnel to perform the measurements, and weather conditions. During these scheduled visits, researchers usually collect fluxes from all three GHGs and analyze them systematically to calculate magnitudes and patterns throughout the experiment. Usually, researchers perform manual samples during the early hours of the day (between 9 am and 12 pm) to avoid confounding effects due to large changes in temperature and moisture, as demonstrated by information summarized by the soil respiration global database (Cueva et al., 2017; Jian et al., 2020). Consequently, we selected subsamples from each original GHG time series (derived from automated measurements) using flux measurements from 10 am at fixed intervals of once per month (n=12), twice per month (n=24), or four times per month (n=48) starting on the first week of available data from automated measurements.

We applied *tuLHs* as an alternative subsampling approach to obtain an optimized subsample with the same univariate statistical properties and temporal dependence relationship of the original GHG time series. Optimization was performed to select subsamples for each GHG flux using the same number of samples as for FTS: twelve (k=12), twenty-four (k=24), or forty-eight (k=48) measurements throughout the year of available data from automated measurements.

2.4 Temporal Univariate Latin Hypercube Sampling (tuLHs)

Let $S = \{(x_1, y_1, z_1), (x_2, y_2, z_2), \ldots, (x_n, y_n, z_n)\}$ be observations of the variables X, Y, and Z in a time series, where X, Y, and Z are soil GHGs (i.e., CO_2, CH_4, and N_2O). Each measured variable is characterized by the univariate probability distribution function and the temporal

dependency function. Once these two functions are known, then the behaviors of the variable can be reproduced (Le et al., 2020; Chilès and Delfiner, 2009; Trangmar et al., 1986; Pyrcz and Deutsch, 2014). The *tuLHs* consists of three steps: (1) modeling the univariate behavior of the variable using the empirical cumulative univariate probability distribution function; (2) modeling the temporal dependence using the empirical variogram function; and (3) optimizing a subsample applying a global optimization method, differential evolution, using the previously obtained variogram function as an objective function.

First, to model the univariate behavior of the variables from the observations of S, the empirical univariate cumulative distribution function $F^*_n(x)$ of X is estimated by:

$$F_n^*(x) = \frac{1}{n}\sum_{i=1}^{n} I\{x_i \leq x\} \quad (1)$$

where *I* represents an indicator function equal to 1 when its argument is true, and 0 otherwise. Similarly, the empirical univariate distribution function of the variables *Y* and *Z* can be derived. Second, to model the temporal dependence of the variables from the observations of *S*, the empirical temporal correlation function (i.e., temporal variogram function) $\gamma^*(t)$ of X is estimated by:

$$\gamma^*(t) = \frac{1}{2N(t)}\sum_{i=1}^{N(t)} [X(t_i + t) - X(t_i)]^2 \quad (2)$$

where *N(t)* is the number of pairs $X(t_i + t)$ *and* $X(t_i)$ are separated by a time *t*. The variogram functions of the variables Y and Z are analogous. Third, to optimize the subsample, it is required to choose the "optimal" data points with the selected sample size (i.e., *k*=12, 24, or 48; where $k << n$) that will have the same behavior as the original observations of *S* (i.e., GHG fluxes derived from automated measurements). To achieve this objective, we use differential evolution, a global optimization method (Storn and Price, 1997), using the variogram function as an objective function. The procedure consists of dividing the univariate empirical probability

187 distribution in Eq. (1) into *k* equiprobable strata, which is equivalent to k ordered data subsets.
188 From each subset, only one value must be chosen to satisfy the condition of a univariate Latin
189 hypercube. The differential evolution method is applied to find the optimal points that
190 minimize the difference between the subsample variogram γ (t) and the data variogram γ * (t)
191 in Eq. (3).

192 $$OF_1 = \sum_{i=1}^{N(t)} [\gamma(t) - \gamma^*(t)]^2 \qquad (3)$$

193 where *OF* is the objective function, and the variograms γ (t) and γ * (t) are calculated using Eq.
194 (2).
195
196 *2.5 Statistical analyses*
197 The t-test was used to compare the means, and the Kolmogorov-Smirnov test was used to
198 compare the probability distribution of measurements derived from each sampling protocol.
199 All tests were done with a 95% confidence level. In addition, their statistical properties, such
200 as mean, median, standard deviation, and first and third quartile, were compared. The
201 differences in the experimental semivariograms were calculated as a comparison measure for
202 the temporal dependence of the samples and the original time series of GHG fluxes. For
203 cumulative sums of GHG flux, their mean is calculated as the most likely value, and their
204 quantile difference between 97.5 and 2.5 is used to quantify the range of uncertainty. All
205 analyzes were performed using the R program (Team and Others, 2013).
206
207 **3. Results**
208 *3.1 Relationships among GHG fluxes from soils*
209 Justification in support of FTS for simultaneous measurements of GHG fluxes would require
210 evidence of strong linear correlations between magnitudes and temporal dependence among

soil GHG fluxes. First, we did not find strong linear relationships between any combination of GHG fluxes from soils derived from automated measurements (Fig. S1). Therefore, our data did not support the assumption that the magnitude of one GHG flux was associated with a linear increase or decrease of another GHG flux. Second, semivariogram models demonstrated differences in the temporal dependence for each GHG flux. Automated measurements of soil CO_2 fluxes (F_ACO_2) showed a temporal dependence following a Gaussian variogram model, with a nugget of 4, a sill plus nugget of 28, and a correlation range of 80 days (Fig. S2a). Automated measurements of soil CH_4 fluxes (F_ACH_4) also showed a temporal dependence but followed a spherical variogram model, with a nugget of $7x10^{-8}$, a sill plus nugget of $1.5x10^{-7}$, and a correlation range of 110 days (Fig. S2b). In contrast, automated measurements of soil N_2O fluxes (F_AN_2O) did not show a temporal dependence, where a pure nugget effect was present, and with a correlation range of 0 days (Fig. S2c). Consequently, these GHG fluxes' magnitudes and temporal patterns were different and did not support FTS for simultaneous measurements of GHG from soils.

3.2 Optimization of GHG sampling protocols

We applied a *tuLHs* approach to identify subsamples with the same statistical properties and temporal dependence for each of the original GHG time series from automated measurements. Subsamples were identified for twelve (k=12), twenty-four (k=24), or forty-eight (k=48) measurements throughout the year for each GHG time series. Our results show that the optimized measurement dates were different for each GHG flux (Fig. 1), and we provide explicit examples for k=24 (Fig. 1) and k=12, 48 (Fig. S3, S4).

The optimized CO_2 subsamples were well distributed throughout the year for all sampling scenarios (i.e., k from 12 to 48) because F_ACO_2 had a strong temporal dependence and a small nugget effect with respect to the sill (Fig. S2a). The optimized CH_4 subsamples

were also relatively well distributed throughout the year, especially for scenarios of k=24 and k=48, as $F_A CH_4$ also had a temporal dependence but with a higher nugget effect with respect to the sill (Fig. S2b). Finally, the optimized N_2O subsamples were more challenging to define, especially with a small sample size (i.e., k=12; Fig. S3c) because $F_A N_2O$ did not have a temporal dependence (Fig. S2c).

3.3 Differences in statistical properties and temporal dependency of subsamples

Overall, there were no statistically significant differences between the mean values derived from automated measurements and those from FTS or the *tuLHs* approach (Fig. 2 for k=24; Fig. S5 for k=12; Fig. S6 for k=48; Tables S1 and S2). Although this appears promising, more than a simple comparison of the means is needed to evaluate the information derived from different sampling approaches. In other words, it is possible to have a similar mean value without reproducing the probability distribution nor the temporal dependence of the original time series (i.e., correct answer but for the wrong reasons). Here, we present results based on comparing the means, standard deviation, probability distributions, and semivariograms derived from automated measurements and the different sampling scenarios for all GHG fluxes.

The mean of $F_A CO_2$ was 5.9 μmol CO_2 m^{-2} s^{-1}, while the mean for FTS 5.5 μmol CO_2 m^{-2} s^{-1} and 5.9 μmol CO_2 m^{-2} s^{-1} for the *tuLHs* approach with k=24 (Fig. 3a-c). These results were comparable with the means derived from FTS (5.4 and 5.4 μmol CO_2 m^{-2} s^{-1}) and the *tuLHs* approach (6.2 and 5.9 μmol CO_2 m^{-2} s^{-1}) using k=12 and k=48, respectively (Figs. S5, S6; Table S1). The standard deviation of $F_A CO_2$ was 3.9 and 3.2 μmol CO_2 m^{-2} s^{-1} for FTS, and 3.9 μmol CO_2 m^{-2} s^{-1} for the *tuLHs* approach with k=24 (Figs. 3a-c). These results were comparable with the standard deviations derived from FTS (3.1 and 3.3 μmol CO_2 m^{-2} s^{-1}) and the *tuLHs* approach (4.1 and 3.9 μmol CO_2 m^{-2} s^{-1}) using k=12 and k=48, respectively (Fig. S5,

S6; Table S1). Our results show that the semivariograms of optimized samples using the *tuLHs* approach closely approximate the semivariograms of automated measurements for k=24 (Fig. 4a) and k=12 and 48 (Figs. S7a, S8a). These results are consistent with the sums of absolute differences between the semivariograms of the samples and the semivariogram of F_ACO_2 with differences of 69.31, 54.39, 49.42 for FTS, and 5.69, 1.99, 1.39 for the *tuLHs* approach for k=12, 24, 48, respectively (Table S2).

The mean of F_ACH_4 was -0.93 nmol CH_4 m^{-2} s^{-1}, while -0.86 nmol CH_4 m^{-2} s^{-1} for FTS and -0.94 nmol CH_4 m^{-2} s^{-1} for the *tuLHs* approach with k=24 (Fig. 3d-f). These results were also comparable with the means derived from FTS (-0.83 and -0.88 nmol CH_4 m^{-2} s^{-1}) and the *tuLHs* approach (-0.87 and -0.92 nmol CH_4 m^{-2} s^{-1}) using k=12 and 48, respectively (Figs. S5, S6; Table S1). The standard deviation of F_ACH_4 was 0.36 and 0.26 nmol CH_4 m^{-2} s^{-1} for FTS and 0.34 nmol CH_4 m^{-2} s^{-1} for the *tuLHs* approach with k=24. These results were comparable with the standard deviations derived from FTS (0.27 and 0.29 nmol CH_4 m^{-2} s^{-1}) and the *tuLHs* approach (0.33 and 0.35 nmol CH_4 m^{-2} s^{-1}) using k=12 and k=48, respectively (Figs. S5, S6; Table S1). The semivariograms of optimized samples using the *tuLHs* approach closely approximate the semivariogram of automated measurements for k=24 (Fig. 4b) and k=12 and 48 (Figs. S7b, S8b). Consequently, the sums of absolute differences between the semivariograms of the samples and the semivariogram of F_ACH_4 were 0.63, 0.48,0.49 for FTS, and 0.06, 0.04, 0.02 for the *tuLHs* approach with k=12, 24, 48, respectively (Table S2).

Finally, the mean of F_AN_2O was 0.45 and 0.61 nmol N_2O m^{-2} s^{-1} for FTS, and 0.51 nmol N_2O m^{-2} s^{-1} for the *tuLHs* approach with k=24 (Fig. 3g-i). These results were also comparable with the means derived from FTS (0.59 and 0.25 nmol N_2O m^{-2} s^{-1}) and the *tuLHs* approach (0.58 and 0.49 nmol N_2O m^{-2} s^{-1}) using k=12 and 48, respectively (Figs. S5, S6; Table S1). The standard deviation of F_AN_2O was 1.62 and 1.97 nmol N_2O m^{-2} s^{-1} for FTS, and 1.54 nmol N_2O m^{-2} s^{-1} for the *tuLHs* approach with k=24. These results were comparable with the standard

deviations derived from FTS (1.38 and 0.91 nmol N_2O m^{-2} s^{-1}) and the *tuLHs* approach (1.58 and 1.54 nmol N_2O m^{-2} s^{-1}) using k=12 and k=48, respectively (Figs. S5, S6; Table S1). Our results show no temporal dependence for N_2O fluxes, but the semivariograms of optimized samples using the *tuLHs* approach closely approximate the semivariogram of automated measurements for k=24 (Fig. 4c) and k=12 and 48 (Figs. S7c, S8c). Consistently, the sum of absolute differences between the semivariograms of the samples and the semivariogram of $F_A N_2O$ were 10.01, 12.25, 16.75 for FTS, and 0.82, 1.13, 3.57 for the *tuLHs* approach with k=12, 24, 48, respectively (Table S2).

These results show that the *tuLHs* approach reproduced the probability distribution and the temporal dependence of the time series derived from automated measurements with more precision than FTS for all GHGs. In the next section, we explore the implications of these differences for calculating cumulative GHG fluxes.

3.4 Calculation of cumulative GHG fluxes

We calculated the cumulative flux for all GHGs using available information from automated measurements (Fig. 2; Table S3). The cumulative sum for available measurements of $F_A CO_2$ was 5758.5 g CO_2 m^{-2} [893.9, 13860.8; 95% CI]; for $F_A CH_4$ was -0.47 g CH_4 m^{-2} [-0.81, -0.19; 95% CI]; and 0.63 g N_2O m^{-2} [-0.75, 5.19; 95% CI] for $F_A N_2O$.

We used the mean for each GHG flux derived from the *tuLHs* approach or the FTS to calculate the cumulative sum (Table S3). We found that the FTS underestimated the cumulative flux (-8.4, -6.2, -7.1%) and the uncertainty (-32.6, -21.6, -19.3%) of $F_A CO_2$ for k=12, 24, 48, respectively (Fig. 5a). In contrast, the *tuLHs* approach slightly overestimated the cumulative flux (6.5, 1.1, 0.1%) and slightly underestimated the uncertainty (-9.1, -4.4, -3.7%) for k=12, 24, 48, respectively (Fig. 5a).

The FTS underestimated the cumulative flux (-9.1, -6.1, -3.1%) and the uncertainty (-31.8, -27.3, -15.9%) of $F_A CH_4$ for k=12, 24, 48, respectively (Fig. 5b). In contrast, the *tuLHs* approach underestimated the cumulative flux (-6.1%) only for k=12, but slightly underestimated the uncertainty (-15.9, -6.8, -4.5%) for k=12, 24, 48, respectively (Fig. 5b).

The FTS substantially underestimated the cumulative flux (-168, -170, -173%) of $F_A N_2O$ for k=12, 24, 48, respectively. Uncertainty was overestimated for k=12 and 24 (3.6 and 26%) and underestimated for k=48 (-31%; Fig. 5c). In contrast, the *tuLHs* approach overestimated less the cumulative flux (29.5, 13.4, 9.1%) for k=12, 24, 48, respectively (Fig. 5c). This approach underestimated the uncertainty for k=12 (-11.2%) and k=24 (-13.8%) but overestimated the uncertainty by 2.9% for k=48 (Fig. 5c). These results show that the *tuLHs* approach consistently provided closer estimates for cumulative sums and uncertainty ranges than an FTS for all GHG fluxes.

4. Discussion

Applied challenges, such as quantifying the role of soils in nature-based solutions, require accurate estimates of GHG fluxes. To do this, two fundamental problems exist for designing environmental monitoring protocols: where and when to measure? Ultimately a monitoring protocol aims to quantify the attributes of an ecosystem so that it can be compared in time within that ecosystem or with other ecosystems. Because we cannot measure everything, everywhere, and all the time, we can argue that any monitoring protocol has assumptions based on physical, economic, social, and practical reasons to address a specific scientific question. These assumptions for designing monitoring protocols could result in misleading, biased, or wrong conclusions, and therefore is critical to assess the consequences of different monitoring efforts. As Hutchinson described in “The Concept of Pattern in Ecology,” we do

not always know if a given pattern is extraordinary or a simple expression of something which we may learn to expect all the time (Hutchinson, 1953).

Automated measurements have revolutionized our understanding of the temporal patterns and magnitudes of soil GHG fluxes (Savage et al., 2014; Bond-Lamberty et al., 2020; Tang et al., 2006; Capooci and Vargas, 2022b). These measurements have limitations in representing spatial variability and have higher equipment costs that limit their broad applicability across study sites (Vargas et al., 2011). Consequently, discrete manual measurements are a common approach to simultaneously measure multiple GHG fluxes and report patterns, budgets, and information to parameterize empirical and process-based models (Phillips et al., 2017; Wang and Chen, 2012). In this study, we argue that the convenience of simultaneously measuring multiple GHGs using FTS may result in biased estimates. Therefore, optimization of sampling protocols is needed to provide insights to improve measurement protocols when there is a limited number of measurements in time (i.e., k=12, 24, 48).

We show that the magnitude of one GHG flux is not associated with a linear increase or decrease of another GHG flux, and the temporal dependencies of each GHG flux are different (Fig. S1). Therefore, it is not possible to infer the dynamics of one GHG flux based solely on information from another under the assumption that they share similar (or autocorrelated) biophysical drivers. These results imply that the magnitudes and temporal patterns of GHGs are different and therefore do not support an FTS approach for simultaneous measurements of GHG fluxes from soils.

Multiple studies have shown that the relevance of different biophysical drivers (e.g., temperature, moisture, light) is different for soil CO_2, CH_4, or N_2O fluxes (Luo et al., 2013; Tang et al., 2006; Ojanen et al., 2010). Our results show that soil CO_2 fluxes have a strong temporal dependence (Fig. S2a), likely due to the strong relationship between these fluxes

359 and soil temperature in this and other temperate mesic ecosystems (Hill et al., 2021; Bahn et
360 al., 2010; Barba et al., 2019). The temporal dependence decreased for soil CH_4 fluxes (Fig.
361 S2b), where there is less evidence for such a strong correlation with soil temperature in this
362 and other temperate mesic ecosystems (Bowden et al., 1998; Castro et al., 1995; Warner et
363 al., 2019; Barba et al., 2019). It has been reported that multiple variables and complex
364 relationships are usually needed to explain the variability of soil CH_4 fluxes in forest soils, as
365 there is a delicate balance between methanogenesis and methanotrophy (Luo et al., 2013;
366 Castro et al., 1994; Murguia-Flores et al., 2018). In contrast, soil N_2O fluxes had no temporal
367 dependence (Fig. S2c), showing decoupling from the observed patterns of soil CO_2 and CH_4
368 fluxes (Wu et al., 2010), likely as a result of independent biophysical drivers regulating soil
369 N_2O fluxes (Luo et al., 2013; Bowden et al., 1993; Ullah and Moore, 2011).
370 To address the limitations of an FTS protocol, we propose a novel optimization
371 approach (i.e., *tuLHs*) to reproduce the probability distribution and the temporal dependence
372 of each original time series of GHG fluxes. Traditional methods usually optimize subsamples
373 by either individually focusing on reproducing the probability distribution of the original
374 information (Huntington and Lyrintzis, 1998) or reproducing the temporal dependence of the
375 original information (Gunawardana et al., 2011). The *tuLHs* is a simple approach that uses
376 the univariate probability distribution function and the temporal correlation function (i.e.,
377 variogram) as objective functions for each GHG flux. Our results show that optimized
378 subsamples do not coincide in time for the three GHGs, suggesting that information should
379 be collected based on each GHG flux's specific statistical and temporal characteristics (Fig.
380 1). This study provides proof-of-concept for the application of the *tuLHs.* It demonstrates
381 how an optimization approach provides insights to design monitoring protocols and improve
382 soil GHG flux estimates.

The more temporal data we can collect, the better, but in many cases, measurement protocols are limited to a few measurements per year (i.e., k=12 to 48). Our results demonstrate that for a small sample size (i.e., k=12), the optimized measurements for soil CO_2 fluxes are consistently spread across the year, and for soil CH_4 fluxes are centered within the growing season because of their strong temporal dependence. For the case of soil N_2O fluxes, the variogram shows a constant temporal variability, meaning there is no temporal dependence. Therefore, the optimized measurements are concentrated within the fall season due to their distribution probability (Fig. 1a). Our optimization approach shows how measurements can be distributed across time as more samples are available (i.e., k=24 to 48; Fig. 1b-c) and demonstrates that optimization is critical when a limited number of measurements are available. In other words, a few measurements properly distributed across time provide better agreement with information derived from automated measurements. A similar conclusion was proposed for the spatial distribution of environmental observatory networks, where a network of few sites properly distributed (e.g., across a country) improves our understanding of the target variable more than a spatially biased network (Villarreal et al., 2019). Thus, the representativeness assessment of information collected across time and space is needed to evaluate environmental measurements and quantify nature-based solutions accurately.

We highlight that this optimization approach should be implemented across different ecosystems as it will result in site-specific recommendations. The *tuLHs* can be applied to any time series length and with any time step (e.g., hours, days), but specific results will be representative of the probability distribution and the temporal dependence of the selected time series. In this case study, the year chosen had typical climatological conditions and demonstrates that the statistical properties of the GHG fluxes are different and do not support an FTS approach. Therefore, longer time series (e.g., multi-year) may provide more robust

optimizations that can be applied to monitoring efforts in future years. Alternatively, forecast scenarios can be predicted, and *tuLHs* can be used to suggest an optimized sampling design under those assumptions. Testing the implications of potentially biased GHG flux estimates should be a priority. Ideally, automated measurements should be co-located with manual efforts to adequately capture the temporal and spatial variability of soil GHG fluxes at a specific site.

There are several implications of biased monitoring protocols for understanding soil GHG fluxes and nature-based solutions. First, temporal patterns and temporal dependency may need to be revisited for studies using an FTS approach. Soil GHG fluxes have complex temporal dynamics that vary from diurnal to seasonal and annual scales that a few measurements following an FTS approach cannot reproduce (Barba et al., 2019; Bréchet et al., 2021). Second, soil GHG fluxes could present hot-moments, which are transient events with disproportionately high values that are often missed with an FTS approach (Vargas et al., 2018; Butterbach-Bahl et al., 2004). Third, cumulative sums and uncertainty ranges are biased or misleading when derived using an FTS approach (Tallec et al., 2019; Lucas-Moffat et al., 2018; Capooci and Vargas, 2022b). Our study demonstrates that an optimized approach consistently provided closer estimates for cumulative sums and uncertainty ranges when compared with automated measurements (Fig. 5). We postulate that representing the variability of soil N_2O fluxes is more sensitive to the FTS approach (>170% and >30% for cumulative sums and uncertainty ranges, respectively) than for soil CH_4 and CO_2 fluxes. Fourth, it is possible that if the information derived from an FTS approach is biased, then functional relationships could also be different from those derived from automated measurements (Capooci and Vargas, 2022a). It has been argued that hypothesis testing and our capability of forecasting responses of soil GHG fluxes to changing climate conditions is also biased with information from the FTS approach (Vicca et al., 2014). Finally, because

soils have a central role in nature-based solutions within countries and across the world (Griscom et al., 2017; Bossio et al., 2020), accurate measurements are required to assess management practices, environmental variability, and the contribution of GHGs from soils.

Conclusion

We highlight that we only sometimes know if a given pattern is extraordinary or a simple expression of something which we may learn to expect all the time (Hutchinson, 1953). Furthermore, the "Knowledge Paradox" has been recognized in soil science, where innovative knowledge has often not been accepted by or implemented in society (Bouma, 2010). Here, we postulate that with emergent technologies, there is a convenience of measuring multiple GHGs from soils; however, few measurements collected at fixed time intervals result in biased estimates.

We recognize that potential measurement bias depends on each GHG flux's magnitudes and temporal patterns and could be site-specific. Nevertheless, evaluations are needed to quantify potential bias in estimates of GHG budgets and information used for model parameterization and environmental assessments. Furthermore, the underlying assumption that each GHG flux responds similarly to biophysical drivers may need to be tested across multiple ecosystems to quantify how few measurements influence our understanding of magnitudes and temporal patterns of soil GHG fluxes.

In this study, we present a proof-of-concept and propose a novel optimization approach (i.e., temporal univariate Latin Hypercube sampling) that can be applied with site-specific information of different ecosystems to improve monitoring efforts and reduce the bias of GHG flux measurements across time. We highlight that constant biased environmental monitoring may provide confirmatory information, which we have learned to

expect, but modifications of monitoring protocols could shed light on new or unexpected patterns. These new patterns are the ones that will test paradigms and push science frontiers.

Data Availability. All data used for this analysis is available at: https://doi.org/10.6084/m9.figshare.19536004.v1. The R code used in this study is available at: https://github.com/vargaslab/temporal-univariate-Latin-Hypercube.git

Author Contributions. R.V. conceived this study, and V.H.L. designed and performed the primary analysis with input from R.V in all phases. R.V. wrote the manuscript with contributions from V.H.L.

Competing Interest Statement. None

Acknowledgments. The authors thank the Delaware National Estuarine Research Reserve (DNERR) and the St Jones Reserve personnel for their support throughout this study. The authors acknowledge the land on which they realized this study as the traditional home of the Lenni-Lenape tribal nation (Delaware nation). This study was funded by a grant from the National Science Foundation (#1652594) and NASA Carbon Monitoring System (80NSSC21K0964).

FIGURES

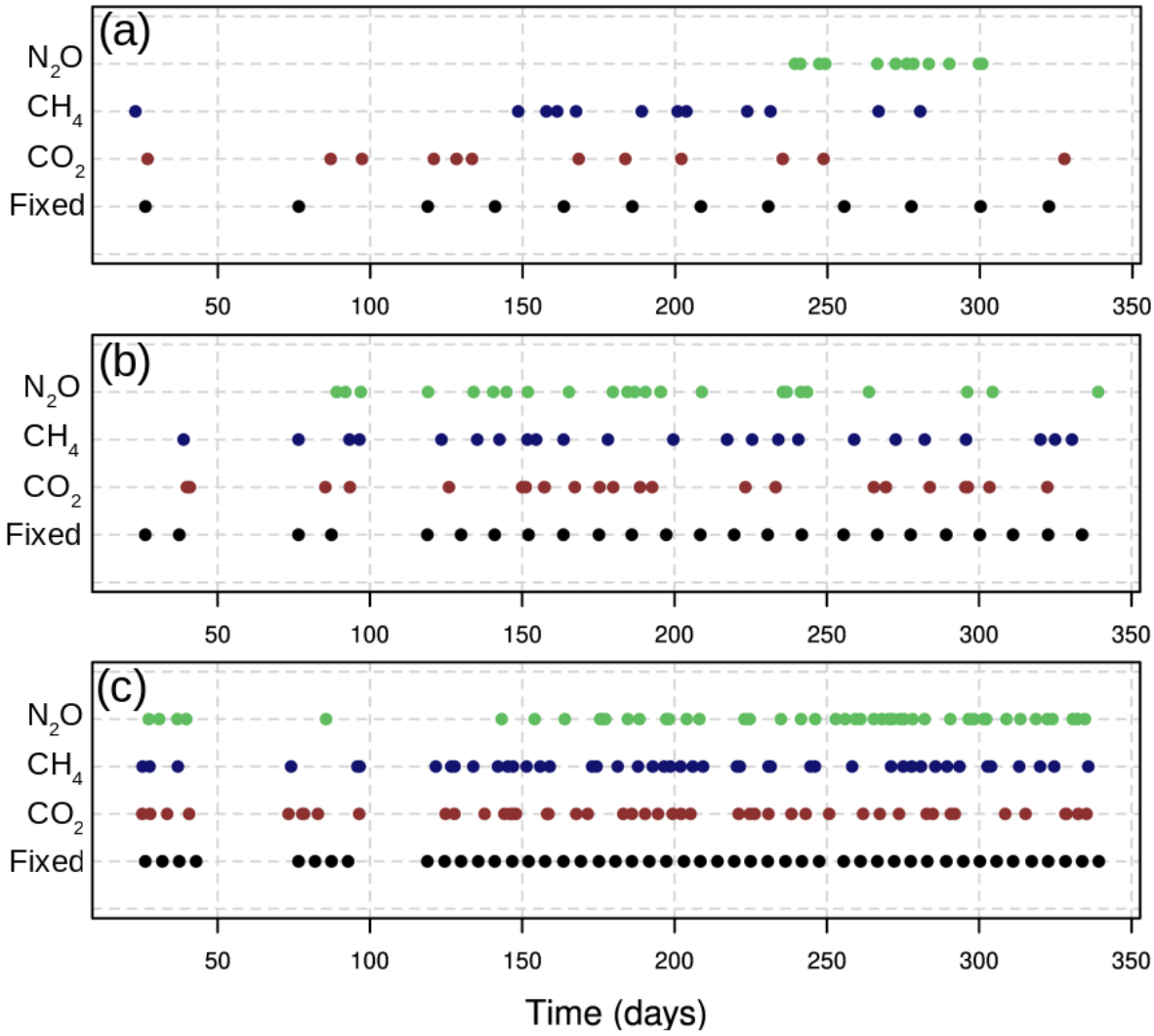

Figure 1. Temporal distribution of fixed temporal stratification (i.e., stratified manual sampling approach) and optimized sampling using a temporal univariate Latin Hypercube (*tuLHs*) approach for: k=12 (a), k=24 (b), and k=48 (c). Fixed temporal stratification is in black, soil CO_2 fluxes in red, soil CH_4 fluxes in blue, and soil N_2O fluxes in green. Time (x-axis) represents days from January 1 to December 31 of, 2015.

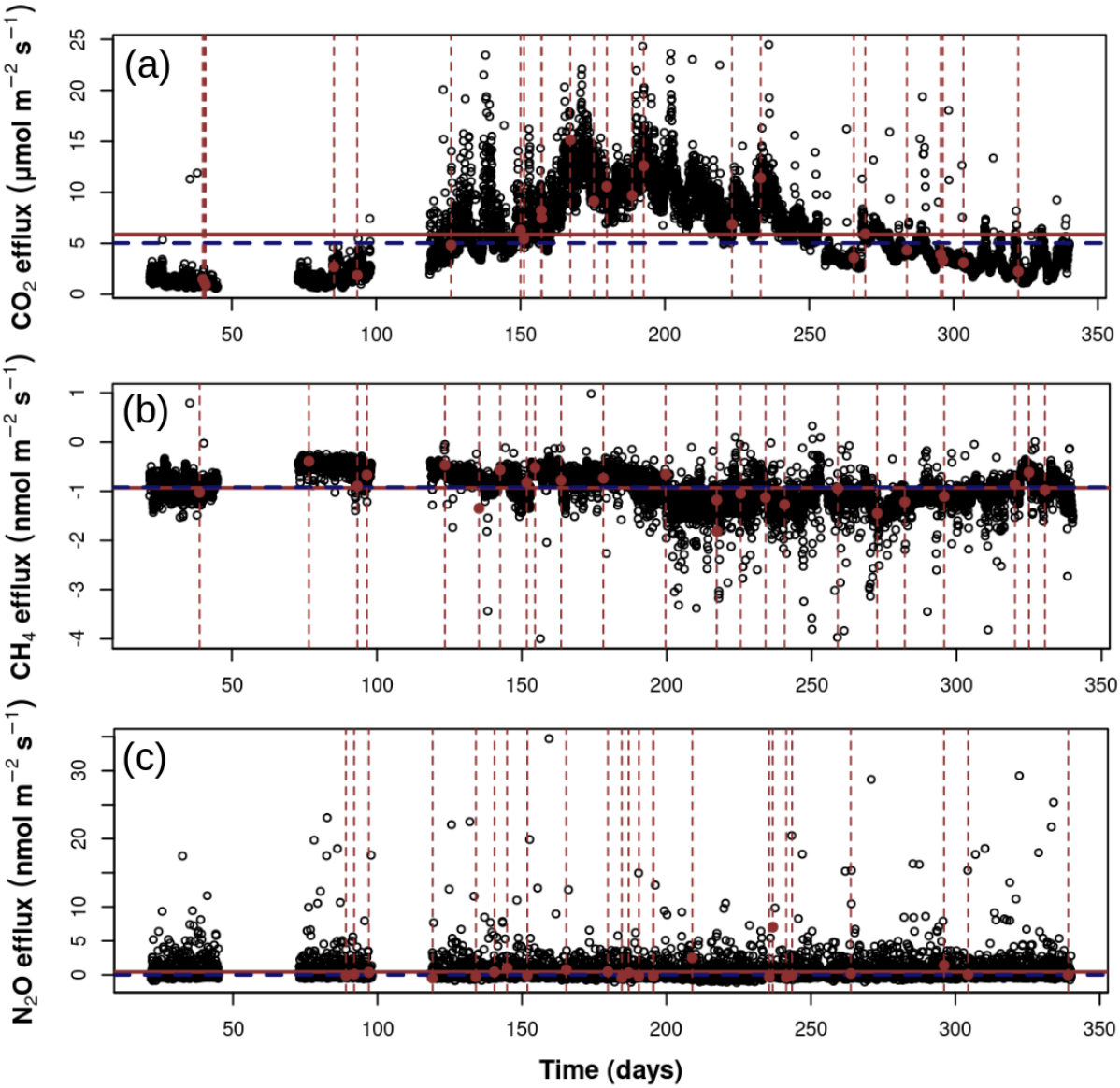

Figure 2. Time series of automated measurements (F_A) of soil greenhouse gas fluxes (black circles) and optimized samples (k=24) using a temporal univariate Latin Hypercube sampling (*tuLHs*) approach for soil CO_2 (a), soil CH_4 (b) and soil N_2O (c) fluxes. The horizontal red line represents the mean, and the horizontal blue line is the median of each greenhouse gas flux derived from automated measurements. The selection of data points for k=12 and 48 are presented for each soil greenhouse gas time series in Figs. S3 and S4, respectively. Time (x-axis) represents days from January 1 to December 31 of, 2015.

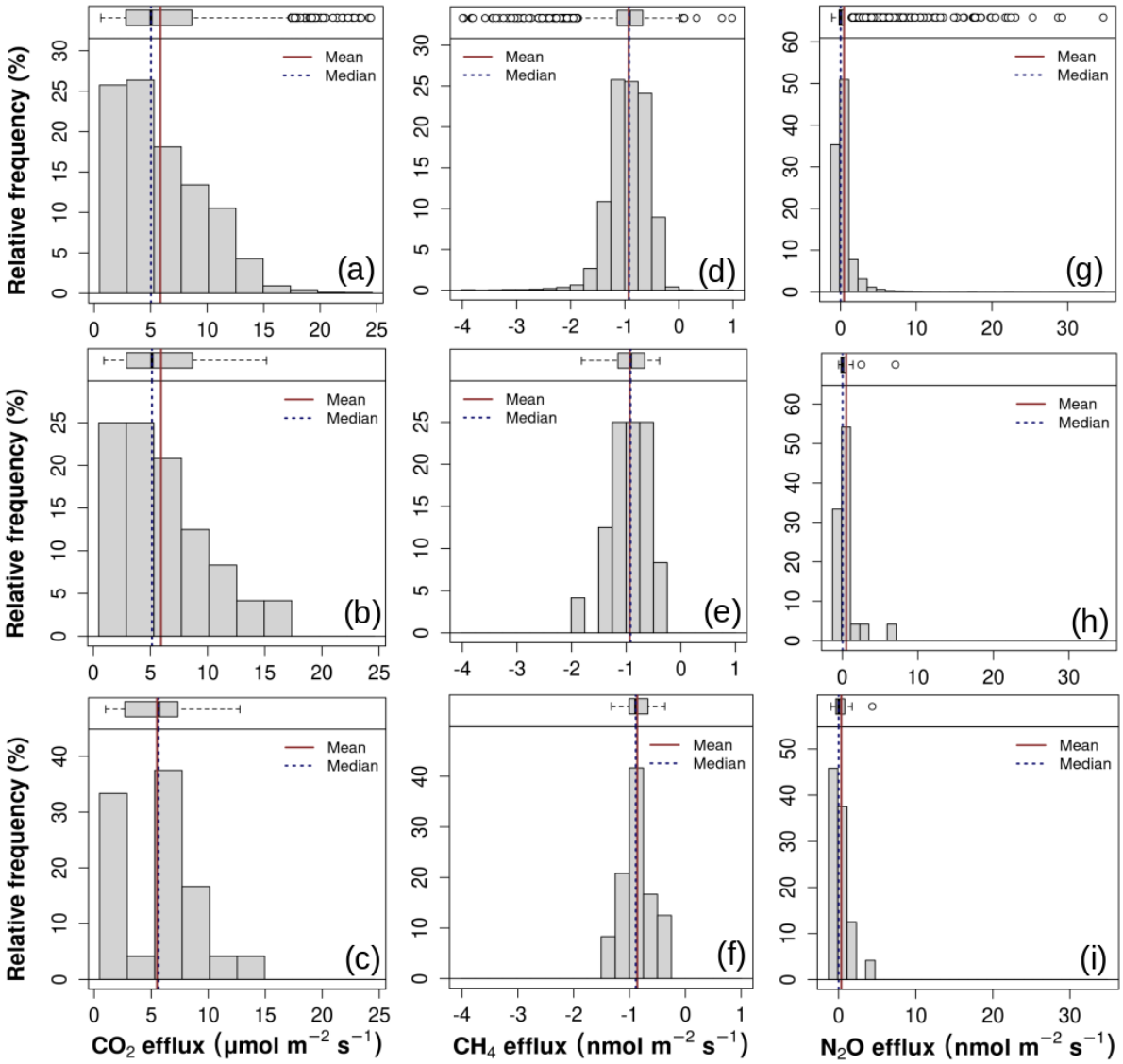

Figure 3. Histograms for automated measurements of soil CO_2 (F_A CO_2; a), soil CH_4 (F_A CH_4; d), and soil N_2O (F_A N_2O; g). Histograms for optimized samples (k=24) using a temporal univariate Latin Hypercube sampling (*tuLHs*) approach for soil CO_2 (b), soil CH_4 (e), and soil N_2O (h) fluxes. Histograms for fixed temporal stratification (i.e., stratified manual sampling schedule) (k=24) for soil CO_2 (c), soil CH_4 (f), and soil N_2O (i) fluxes. Supplementary material includes results for measurements with k=12 (Fig. S5) and k=48 (Fig. S6).

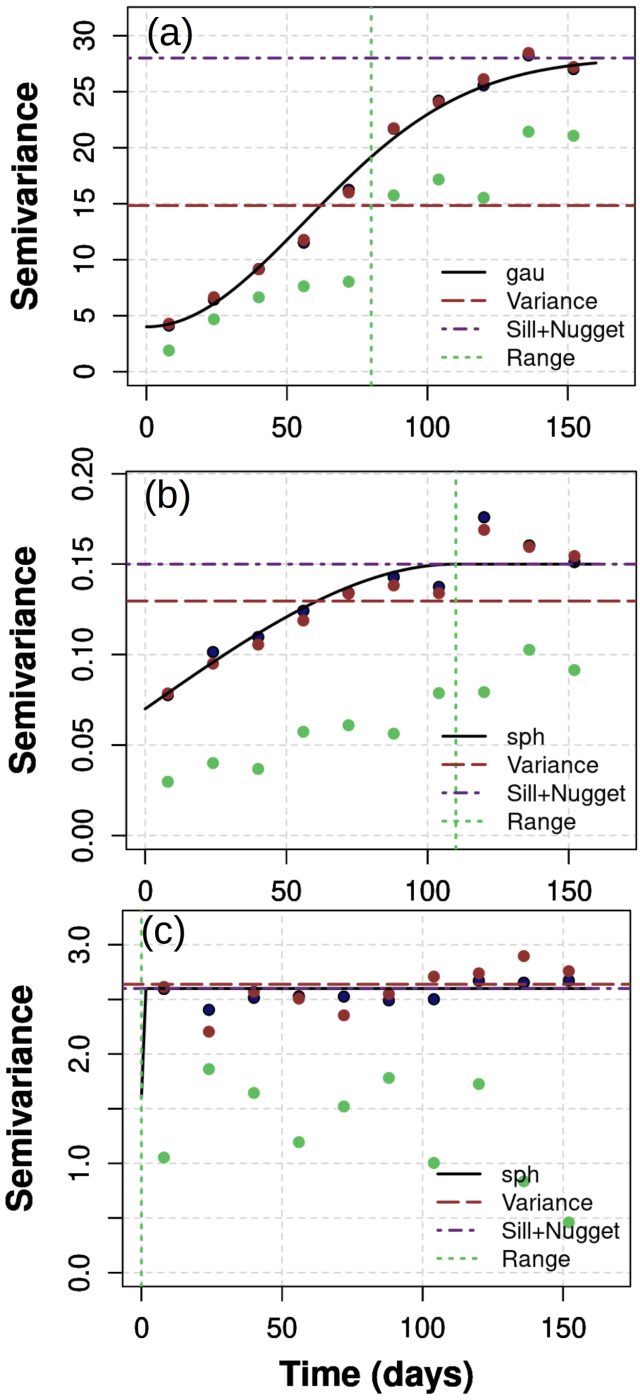

Figure 4. Comparison of semivariograms between automated measurements (F_A) of soil greenhouse gas fluxes (solid black line) and for optimized samples using a temporal univariate Latin Hypercube sampling (*tuLHs*) approach (red circles) or fixed temporal stratification (green circles) with k=24. Semivarograms are presented for soil CO_2 (a), CH_4 (d), and N_2O (c) fluxes. Semivariograms for measurements with k=12 and k=48 are shown in Supplementary Figs. S7 and S8, respectively. Semivariogram fits were gaussian (Gau) or spherical (sph).

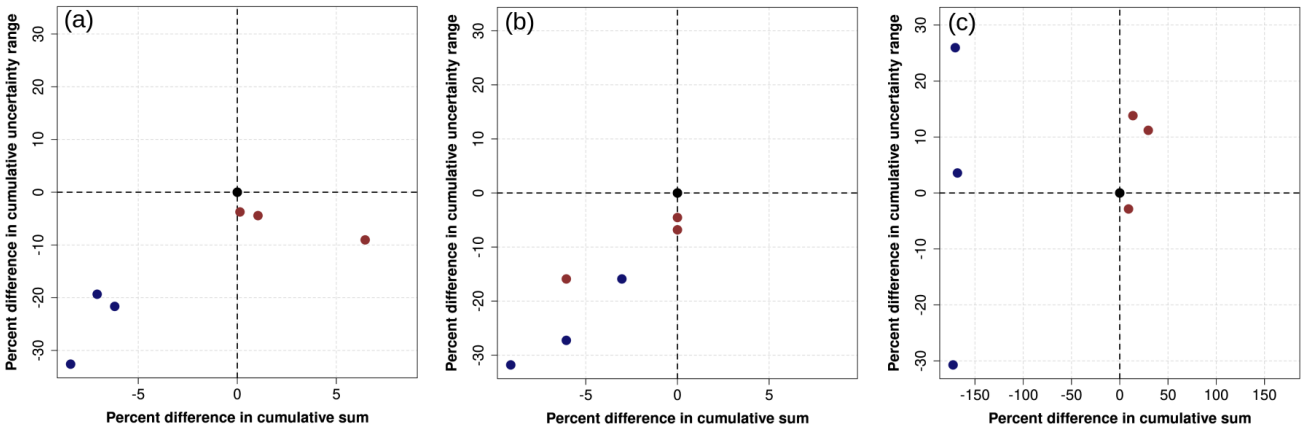

Figure 5. Comparison of percent differences from cumulative sums and associated uncertainty (95% CI) between greenhouse gas fluxes derived from automated measurements (F_A) and using an optimized sampling approach (*tuLHs*) or a fixed temporal stratification. Differences are represented for soil CO_2 (a), soil CH_4 (b), and soil N_2O (c) fluxes. The black circle in the center (0,0) of a plot represents the values derived from automated measurements (F_A). Blue circles represent estimates from fixed temporal stratification, and red circles represent estimates from an optimized sampling approach (*tuLHs*). Estimates were calculated based on the 258 available automated measurements (Fig. 2), and numeric estimates are in Table S3.

References

Bahn, M., Reichstein, M., Davidson, E. A., Gruenzweig, J., Jung, M., Carbone, M. S., Epron, D., Misson, L., Nouvellon, Y., Roupsard, O., Savage, K., Trumbore, S. E., Gimeno, C., Curiel Yuste, J., Tang, J., Vargas, R., and Janssens, I. A.: Soil respiration at mean annual temperature predicts annual total across vegetation types and biomes, Biogeosciences, 7, 2147–2157, 2010.

Ball, B. C.: Soil structure and greenhouse gas emissions: a synthesis of 20 years of experimentation, Eur. J. Soil Sci., 64, 357–373, 2013.

Barba, J., Poyatos, R., and Vargas, R.: Automated measurements of greenhouse gases fluxes from tree stems and soils: magnitudes, patterns and drivers, Sci. Rep., 9, 4005, 2019.

Barba, J., Poyatos, R., Capooci, M., and Vargas, R.: Spatiotemporal variability and origin of CO2 and CH4 tree stem fluxes in an upland forest, Glob. Chang. Biol., 27, 4879–4893, 2021.

Bond-Lamberty, B., Christianson, D. S., Malhotra, A., Pennington, S. C., Sihi, D., AghaKouchak, A., Anjileli, H., Altaf Arain, M., Armesto, J. J., Ashraf, S., Ataka, M., Baldocchi, D., Andrew Black, T., Buchmann, N., Carbone, M. S., Chang, S., Crill, P., Curtis, P. S., Davidson, E. A., Desai, A. R., Drake, J. E., El-Madany, T. S., Gavazzi, M., Görres, C., Gough, C. M., Goulden, M., Gregg, J., Gutiérrez del Arroyo, O., He, J., Hirano, T., Hopple, A., Hughes, H., Järveoja, J., Jassal, R., Jian, J., Kan, H., Kaye, J., Kominami, Y., Liang, N., Lipson, D., Macdonald, C. A., Maseyk, K., Mathes, K., Mauritz, M., Mayes, M. A., McNulty, S., Miao, G., Migliavacca, M., Miller, S., Miniat, C. F., Nietz, J. G., Nilsson, M. B., Noormets, A., Norouzi, H., O'Connell, C. S., Osborne, B., Oyonarte, C., Pang, Z., Peichl, M., Pendall, E., Perez-Quezada, J. F., Phillips, C. L., Phillips, R. P., Raich, J. W., Renchon, A. A., Ruehr, N. K., Sánchez-Cañete, E. P., Saunders, M., Savage, K. E., Schrumpf, M.,

Scott, R. L., Seibt, U., Silver, W. L., Sun, W., Szutu, D., Takagi, K., Takagi, M., Teramoto, M., Tjoelker, M. G., Trumbore, S., Ueyama, M., Vargas, R., Varner, R. K., Verfaillie, J., Vogel, C., Wang, J., Winston, G., Wood, T. E., Wu, J., Wutzler, T., Zeng, J., Zha, T., Zhang, Q., and Zou, J.: COSORE: A community database for continuous soil respiration and other soil-atmosphere greenhouse gas flux data, Glob. Chang. Biol., 249, 434, 2020.

Bossio, D. A., Cook-Patton, S. C., Ellis, P. W., Fargione, J., Sanderman, J., Smith, P., Wood, S., Zomer, R. J., von Unger, M., Emmer, I. M., and Griscom, B. W.: The role of soil carbon in natural climate solutions, Nature Sustainability, 3, 391–398, 2020.

Bouma, J.: Chapter 4 - Implications of the Knowledge Paradox for Soil Science, in: Advances in Agronomy, vol. 106, edited by: Sparks, D. L., Academic Press, 143–171, 2010.

Bowden, R. D., Castro, M. S., Melillo, J. M., Steudler, P. A., and Aber, J. D.: Fluxes of greenhouse gases between soils and the atmosphere in a temperate forest following a simulated hurricane blowdown, Biogeochemistry, 21, 61–71, 1993.

Bowden, R. D., Newkirk, K. M., and Rullo, G. M.: Carbon dioxide and methane fluxes by a forest soil under laboratory-controlled moisture and temperature conditions, Soil Biol. Biochem., 30, 1591–1597, 1998.

Bréchet, L. M., Daniel, W., Stahl, C., Burban, B., Goret, J.-Y., Salomón, R. L., and Janssens, I. A.: Simultaneous tree stem and soil greenhouse gas (CO2 , CH4 , N2 O) flux measurements: a novel design for continuous monitoring towards improving flux estimates and temporal resolution, New Phytol., 230, 2487–2500, 2021.

588 Butterbach-Bahl, K., Kock, M., Willibald, G., Hewett, B., Buhagiar, S., Papen, H., and Kiese,
589 R.: Temporal variations of fluxes of NO, NO2, N2O, CO2, and CH4in a tropical rain forest
590 ecosystem, Global Biogeochem. Cycles, 18, https://doi.org/10.1029/2004gb002243, 2004.

591 Capooci, M. and Vargas, R.: Diel and seasonal patterns of soil CO2 efflux in a temperate
592 tidal marsh, Sci. Total Environ., 802, 149715, 2022a.

593 Capooci, M. and Vargas, R.: Trace gas fluxes from tidal salt marsh soils: implications for
594 carbon--sulfur biogeochemistry, Biogeosciences, 19, 4655–4670, 2022b.

595 Capooci, M., Barba, J., Seyfferth, A. L., and Vargas, R.: Experimental influence of storm-
596 surge salinity on soil greenhouse gas emissions from a tidal salt marsh, Sci. Total Environ.,
597 686, 1164–1172, 2019.

598 Castro, M. S., Melillo, J. M., Steudler, P. A., and Chapman, J. W.: Soil moisture as a
599 predictor of methane uptake by temperate forest soils, Can. J. For. Res., 24, 1805–1810,
600 1994.

601 Castro, M. S., Steudler, P. A., Melillo, J. M., Aber, J. D., and Bowden, R. D.: Factors
602 controlling atmospheric methane consumption by temperate forest soils, Global Biogeochem.
603 Cycles, 9, 1–10, 1995.

604 Chilès, J.-P. and Delfiner, P.: Geostatistics: Modeling Spatial Uncertainty, John Wiley &
605 Sons, 720 pp., 2009.

606 Cueva, A., Bullock, S. H., López-Reyes, E., and Vargas, R.: Potential bias of daily soil CO2
607 efflux estimates due to sampling time, Sci. Rep., 7, 11925, 2017.

Freeman, C., Lock, M. A., and Reynolds, B.: Fluxes of CO2, CH4 and N2O from a Welsh peatland following simulation of water table draw-down: Potential feedback to climatic change, Biogeochemistry, 19, https://doi.org/10.1007/bf00000574, 1993.

Griscom, B. W., Adams, J., Ellis, P. W., Houghton, R. A., Lomax, G., Miteva, D. A., Schlesinger, W. H., Shoch, D., Siikamäki, J. V., Smith, P., Woodbury, P., Zganjar, C., Blackman, A., Campari, J., Conant, R. T., Delgado, C., Elias, P., Gopalakrishna, T., Hamsik, M. R., Herrero, M., Kiesecker, J., Landis, E., Laestadius, L., Leavitt, S. M., Minnemeyer, S., Polasky, S., Potapov, P., Putz, F. E., Sanderman, J., Silvius, M., Wollenberg, E., and Fargione, J.: Natural climate solutions, Proc. Natl. Acad. Sci. U. S. A., 114, 11645–11650, 2017.

Gunawardana, A., Meek, C., and Xu, P.: A model for temporal dependencies in event streams, Adv. Neural Inf. Process. Syst., 24, 2011.

Hao, W. M., Scharffe, D., Crutzen, P. J., and Sanhueza, E.: Production of N2O, CH4, and CO2 from soils in the tropical savanna during the dry season, J. Atmos. Chem., 7, 93–105, 1988.

Hill, A. C., Barba, J., Hom, J., and Vargas, R.: Patterns and drivers of multi-annual CO2 emissions within a temperate suburban neighborhood, Biogeochemistry, 152, 35–50, 2021.

Huntington, D. E. and Lyrintzis, C. S.: Improvements to and limitations of Latin hypercube sampling, Probab. Eng. Mech., 13, 245–253, 1998.

Hutchinson, G. E.: The Concept of Pattern in Ecology, Proceedings of the Academy of Natural Sciences of Philadelphia, 105, 1–12, 1953.

629 Jian, J., Vargas, R., Anderson-Teixeira, K., Stell, E., Herrmann, V., Horn, M., Kholod, N.,
630 Manzon, J., Marchesi, R., Paredes, D., and Bond-Lamberty, B.: A restructured and updated
631 global soil respiration database (SRDB-V5), Data, Algorithms, and Models,
632 https://doi.org/10.5194/essd-2020-136, 2020.

633 Keller, M., Kaplan, W. A., and Wofsy, S. C.: Emissions of N2O, CH4 and CO2 from tropical
634 forest soils, J. Geophys. Res., 91, 11791, 1986.

635 Kim, D. G., Vargas, R., Bond-Lamberty, B., and Turetsky, M. R.: Effects of soil rewetting
636 and thawing on soil gas fluxes: a review of current literature and suggestions for future
637 research, Biogeosciences, 9, 2459–2483, 2012.

638 Le, V. H., Díaz-Viera, M. A., Vázquez-Ramírez, D., del Valle-García, R., Erdely, A., and
639 Grana, D.: Bernstein copula-based spatial cosimulation for petrophysical property prediction
640 conditioned to elastic attributes, J. Pet. Sci. Eng., 193, 107382, 2020.

641 Lucas-Moffat, A. M., Huth, V., Augustin, J., Brümmer, C., Herbst, M., and Kutsch, W. L.:
642 Towards pairing plot and field scale measurements in managed ecosystems: Using eddy
643 covariance to cross-validate CO2 fluxes modeled from manual chamber campaigns, Agric.
644 For. Meteorol., 256–257, 362–378, 2018.

645 Luo, G. J., Kiese, R., Wolf, B., and Butterbach-Bahl, K.: Effects of soil temperature and
646 moisture on methane uptake and nitrous oxide emissions across three different ecosystem
647 types, Biogeosciences, 10, 3205–3219, 2013.

648 Murguia-Flores, F., Arndt, S., Ganesan, A. L., Murray-Tortarolo, G., and Hornibrook, E. R.
649 C.: Soil Methanotrophy Model (MeMo v1.0): a process-based model to quantify global
650 uptake of atmospheric methane by soil, Geosci. Model Dev., 11, 2009–2032, 2018.

651 Oertel, C., Matschullat, J., Zurba, K., Zimmermann, F., and Erasmi, S.: Greenhouse gas
652 emissions from soils—A review, Geochem. Explor. Environ. Analy., 76, 327–352, 2016.

653 Ojanen, P., Minkkinen, K., Alm, J., and Penttilä, T.: Soil–atmosphere CO2, CH4 and N2O
654 fluxes in boreal forestry-drained peatlands, For. Ecol. Manage., 260, 411–421, 2010.

655 Petrakis, S., Seyfferth, A., Kan, J., Inamdar, S., and Vargas, R.: Influence of experimental
656 extreme water pulses on greenhouse gas emissions from soils, Biogeochemistry, 133, 147–
657 164, 2017.

658 Petrakis, S., Barba, J., Bond-Lamberty, B., and Vargas, R.: Using greenhouse gas fluxes to
659 define soil functional types, Plant Soil, 423, 285–294, 2018.

660 Phillips, C. L., Bond-Lamberty, B., Desai, A. R., Lavoie, M., Risk, D., Tang, J. W., Todd-
661 Brown, K., and Vargas, R.: The value of soil respiration measurements for interpreting and
662 modeling terrestrial carbon cycling, Plant Soil, 413, 1–25, 2017.

663 Pyrcz, M. J. and Deutsch, C. V.: Geostatistical Reservoir Modeling, OUP USA, 433 pp.,
664 2014.

665 Rowlings, D. W., Grace, P. R., Kiese, R., and Weier, K. L.: Environmental factors
666 controlling temporal and spatial variability in the soil-atmosphere exchange of CO2, CH4
667 and N2O from an Australian subtropical rainforest, Glob. Chang. Biol., 18, 726–738, 2012.

668 Savage, K., Phillips, R., and Davidson, E.: High temporal frequency measurements of
669 greenhouse gas emissions from soils, Biogeosciences, 11, 2709–2720, 2014.

670 Shakoor, A., Shahbaz, M., Farooq, T. H., Sahar, N. E., Shahzad, S. M., Altaf, M. M., and
671 Ashraf, M.: A global meta-analysis of greenhouse gases emission and crop yield under no-
672 tillage as compared to conventional tillage, Sci. Total Environ., 750, 142299, 2021.

673 Storn, R. and Price, K.: Differential Evolution – A Simple and Efficient Heuristic for global
674 Optimization over Continuous Spaces, J. Global Optimiz., 11, 341–359, 1997.

675 Tallec, T., Brut, A., Joly, L., Dumelié, N., Serça, D., Mordelet, P., Claverie, N., Legain, D.,
676 Barrié, J., Decarpenterie, T., Cousin, J., Zawilski, B., Ceschia, E., Guérin, F., and Le Dantec,
677 V.: N2O flux measurements over an irrigated maize crop: A comparison of three methods,
678 Agric. For. Meteorol., 264, 56–72, 2019.

679 Tang, X., Liu, S., Zhou, G., Zhang, D., and Zhou, C.: Soil-atmospheric exchange of CO2 ,
680 CH4 , and N2 O in three subtropical forest ecosystems in southern China, Glob. Chang. Biol.,
681 12, 546–560, 2006.

682 Team, RC and Others: R: A language and environment for statistical computing, 2013.

683 Trangmar, B. B., Yost, R. S., and Uehara, G.: Application of Geostatistics to Spatial Studies
684 of Soil Properties, in: Advances in Agronomy, vol. 38, edited by: Brady, N. C., Academic
685 Press, 45–94, 1986.

686 Ullah, S. and Moore, T. R.: Biogeochemical controls on methane, nitrous oxide, and carbon
687 dioxide fluxes from deciduous forest soils in eastern Canada, J. Geophys. Res., 116,
688 https://doi.org/10.1029/2010jg001525, 2011.

689 Vargas, R.: How a hurricane disturbance influences extreme CO2 fluxes and variance in a
690 tropical forest, Environ. Res. Lett., 2012.

691 Vargas, R., Carbone, M. S., Reichstein, M., and Baldocchi, D. D.: Frontiers and challenges in
692 soil respiration research: from measurements to model-data integration, Biogeochemistry,
693 102, 1–13, 2011.

694 Vargas, R., Sánchez-Cañete P., E., Serrano-Ortiz, P., Curiel Yuste, J., Domingo, F., López-
695 Ballesteros, A., and Oyonarte, C.: Hot-Moments of Soil CO2 Efflux in a Water-Limited
696 Grassland, Soil Systems, 2, 47, 2018.

697 Vicca, S., Bahn, M., Estiarte, M., van Loon, E. E., Vargas, R., Alberti, G., Ambus, P., Arain,
698 M. A., Beier, C., Bentley, L. P., Borken, W., Buchmann, N., Collins, S. L., de Dato, G.,
699 Dukes, J. S., Escolar, C., Fay, P., Guidolotti, G., Hanson, P. J., Kahmen, A., Kröel-Dulay, G.,
700 Ladreiter-Knauss, T., Larsen, K. S., Lellei-Kovacs, E., Lebrija-Trejos, E., Maestre, F. T.,
701 Marhan, S., Marshall, M., Meir, P., Miao, Y., Muhr, J., Niklaus, P. A., Ogaya, R., Peñuelas,
702 J., Poll, C., Rustad, L. E., Savage, K., Schindlbacher, A., Schmidt, I. K., Smith, A. R., Sotta,
703 E. D., Suseela, V., Tietema, A., van Gestel, N., van Straaten, O., Wan, S., Weber, U., and
704 Janssens, I. A.: Can current moisture responses predict soil CO2 efflux under altered
705 precipitation regimes? A synthesis of manipulation experiments, Biogeosciences, 11, 2991–
706 3013, 2014.

707 Villarreal, S., Guevara, M., Alcaraz-Segura, D., and Vargas, R.: Optimizing an
708 Environmental Observatory Network Design Using Publicly Available Data, J. Geophys.
709 Res. Biogeosci., 124, 1812–1826, 2019.

710 Wang, G. and Chen, S.: A review on parameterization and uncertainty in modeling
711 greenhouse gas emissions from soil, Geoderma, 170, 206–216, 2012.

712 Warner, D. L., Guevara, M., Inamdar, S., and Vargas, R.: Upscaling soil-atmosphere CO2
713 and CH4 fluxes across a topographically complex forested landscape, Agricultural and forest,
714 264, 80–91, 2019.

Werner, C., Kiese, R., and Butterbach-Bahl, K.: Soil-atmosphere exchange of N2O, CH4, and CO2and controlling environmental factors for tropical rain forest sites in western Kenya, J. Geophys. Res., 112, https://doi.org/10.1029/2006jd007388, 2007.

Wu, X., Brüggemann, N., Gasche, R., Shen, Z., Wolf, B., and Butterbach-Bahl, K.: Environmental controls over soil-atmosphere exchange of N2O, NO, and CO2in a temperate Norway spruce forest, Global Biogeochem. Cycles, 24, https://doi.org/10.1029/2009gb003616, 2010.

Yao, Z., Zheng, X., Xie, B., Liu, C., Mei, B., Dong, H., Butterbach-Bahl, K., and Zhu, J.: Comparison of manual and automated chambers for field measurements of N2O, CH4, CO2 fluxes from cultivated land, Atmos. Environ., 43, 1888–1896, 2009.